Sub-Barrier Fusion Studies Using the LNL Recoil Mass Spectrometer CAMEL.

P. Spolaore

Istituto Nazionale di Fisica Nucleare, Laboratori Nazionali di Legnaro,
Via Romea, 4, 35020 Legnaro (PD), Italy

1. Introduction.

Sub-Barrier fusion has become a rather wide research field since the early discovery, some 10 years ago, that for some heavy nuclei interacting at energies below the Coulomb barrier the probability of fusion reactions is enhanced by orders of magnitude with respect to the expectations based on traditional one-dimensional barrier penetration models.

So far observed experimental evidences of the phenomenon include, in addition to σ_{fus} enhancement (fig. 1 shows results for some Ni+Ni and Ni+Ge systems [1]), an average angular momentum <l> of the compound nucleus larger then predicted by standard barrier penetration models and also exhibiting a characteristic "bump" just below the Coulomb barrier (e.g. fig. 2 [2]), and a corresponding distribution of spins $\sigma(l)$ that extends to partial waves higher then expected on the base of such models (e.g. fig. 3, [3]). Notable isotopic effects are also observed (see fig. 1).

Theoretical description of the data has been in many cases successful within the coupled channel formalism, where the relative motion of the colliding nuclei is coupled to various inelastic and transfer channel states [4], [5], [6]. But there are still open problems, as in some cases a comprehensive description of the cross section and angular momenta (spin) distributions by one model with a fixed set of parameters has failed [7], [8]. Systematic comparison of existing data shows a larger discrepancy between theory and measurement for more symmetric and/or heavy systems (fig. 4, [9]). Reviews on the subject are given, e.g., by Beckerman [10] and Vandenbosch [11].

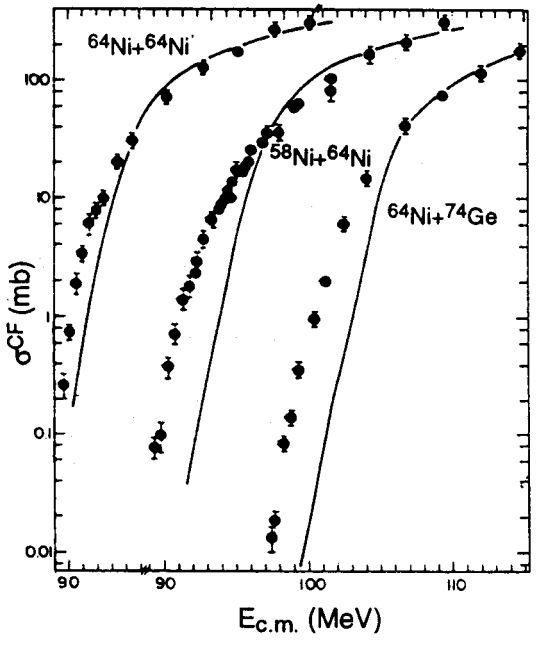

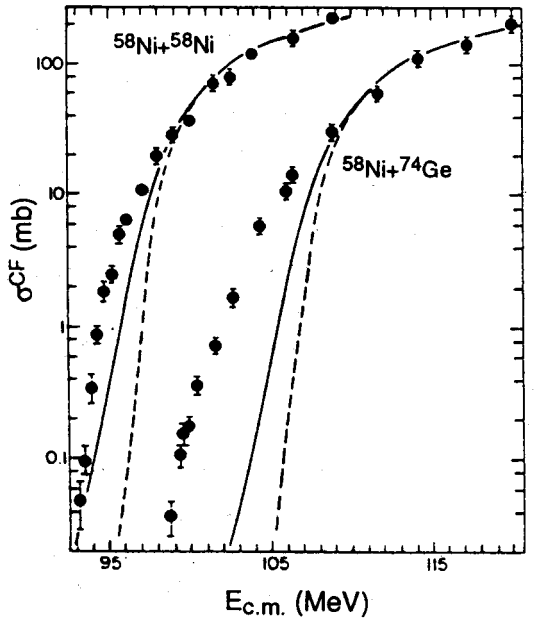

Fig. 1. Fusion cross section data compared with predictions from single barrier penetration models [1].

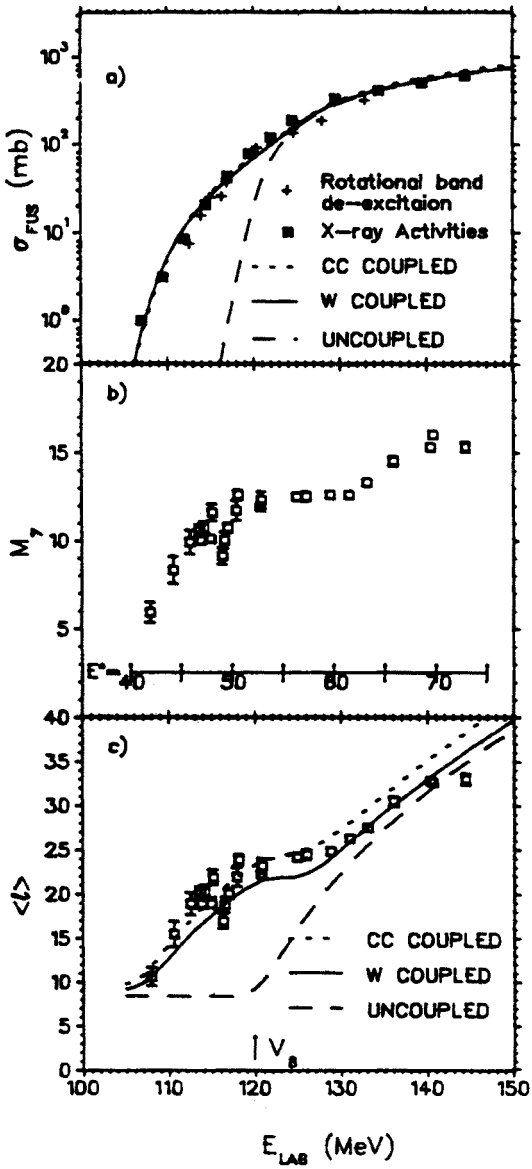

Fig. 2. Fusion excitation function (a), γ-multiplicities (b) and correspondingly deduced average angular momenta (c) for the system $^{28}Si+^{154}Sm$; comparison with Wong model predictions with and without channel coupling [2].

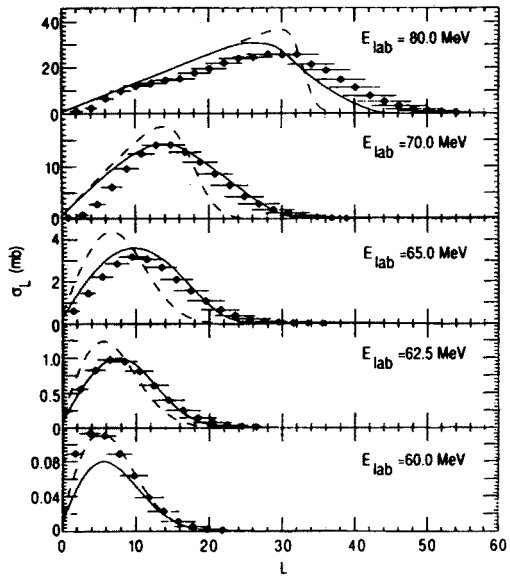

Fig. 3. Angular momentum distributions obtained from γ-multiplicities; solid and dashed curves are the result of calculations performed with coupled-channels and barrier penetration models [3].

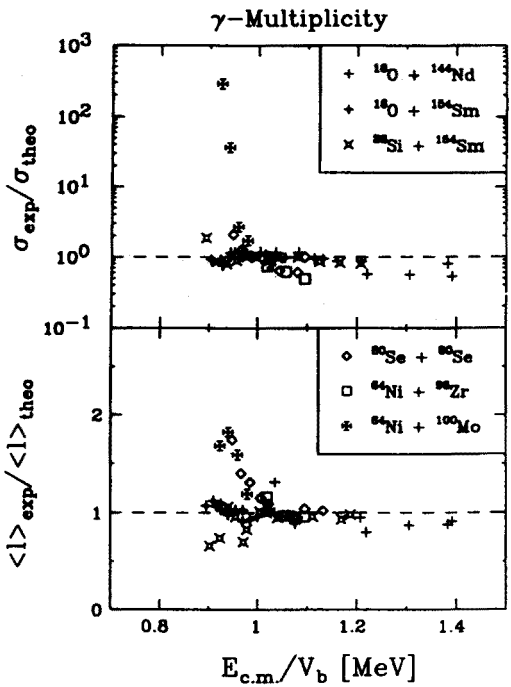

Fig. 4. Ratio of experimental to theoretical fusion cross sections and average angular momenta as a function of bombarding energy relative to the Coulomb barrier for the indicated systems [9].

More recent theoretical analyses of the phenomena bring in concepts like the co-existence of a distribution of potential barriers, and favoured neutron(s) flow at relatively large inter-nuclei distances inducing a "neck" between the two interacting nuclei [12], [13], [14], [15].

The study of this subject is especially interesting as it correlates nuclear reaction dynamics with nuclear structure and the description of the nuclear potential.

On the experimental side there are various quantities that can be measured ($\sigma(E)$, $\sigma(l)$, $\langle l \rangle$, $\langle l^2 \rangle$), relative to the fusion process and also to coupled reaction channels (transfer, etc.), in order to obtain information to test the proposed theoretical descriptions. Especially useful is the measurement of all the different observables relative to the interaction of the same, selected, system(s). The use of one experimental set-up to perform the different measurements may have advantages from the point of view of self-consistency of the data and time consumption.

The need of investigating the fusion reaction down to energies far below the Coulomb barrier makes it very desirable to have apparatus efficiency and selectivity both as high as possible. Of course these two aspects are typically in conflict.

In the following sections a description will be given of an apparatus and the measurement methods used and under development at the Laboratori Nazionali di Legnaro to investigate sub-barrier fusion phenomena.

2. The Apparatus.

An experimental set-up has been developed (and is being improved) at the L.N.L. around the recoil mass spectrometer CAMEL [16] (fig. 5) which is especially suited for measurements with heavy ion fusion reactions.

The spectrometer is composed of two magnetic quadrupole lenses (Q), two electrostatic dipoles (E), one magnetic dipole (M) and two sextupole lenses (S), in the sequence $QQESMSE$. The combination of electric and magnetic dipole fields provides a dispersion of the transmitted particles proportional to the mass to charge ratio m/q, with cancellation of the energy dispersion and isochronous trajectories for each m/q value.

As the incident beam particles and the fusion-evaporation residues have very nearly the same momentum and usually quite different mass (except for extreme cases of very asymmetric inverse reactions) they also have quite different electric rigidities, and are therefore better separated in an electric rather than

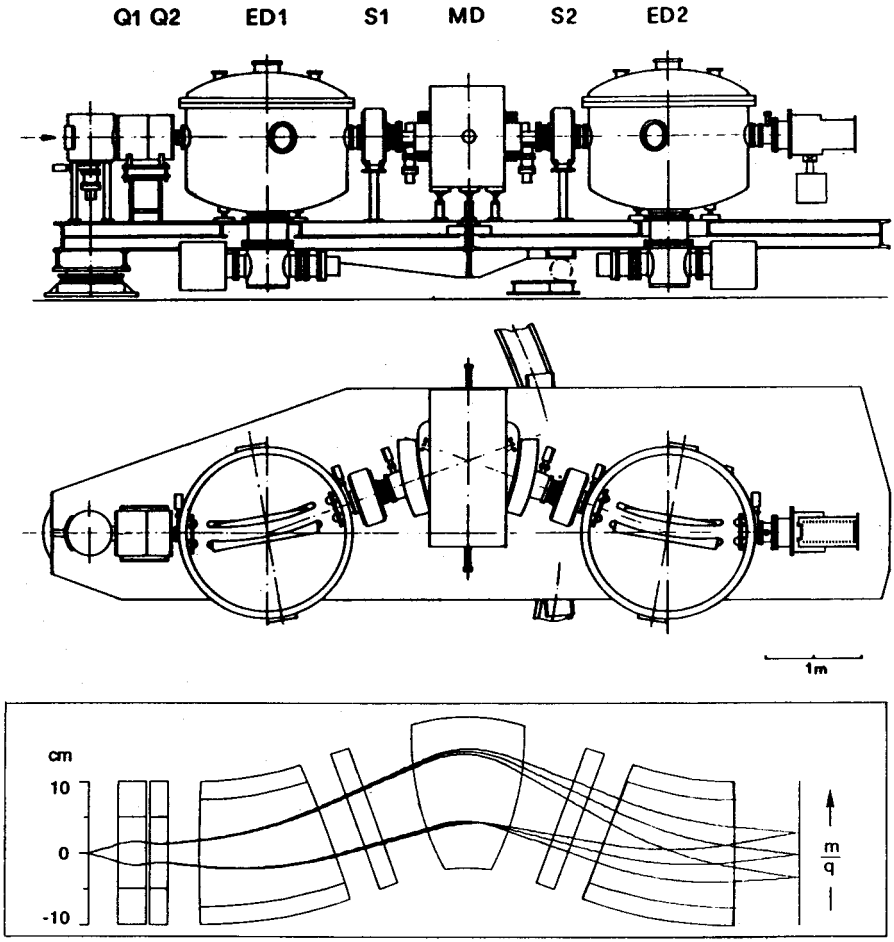

Fig. 5. Lay-out of the CAMEL ("Cross Analyzer of Mass and Energy on-Line") recoil mass spectrometer and sketch of the optical transport.

magnetic field. Including two electrostatic deflectors, the spectrometer can be operated at 0° to the beam direction, where the fusion products density is higher, still providing rather good separation of the forward scattered beam. In addition CAMEL can rotate around the target position from +5° to -55°.

The design of CAMEL was especially aimed to obtain large acceptances for important physical parameters of the analyzed particles beam: $\Delta E/E_0 \approx 40\%$, $\Delta(m/q)/(m_0/q_0) \approx 15\%$, solid angle $\Omega > 10$ msr, with respect to the reference central trajectory of energy E_0, mass m_0, charge state q_0 and zero initial angle and position. The angular acceptance is asymmetric, with a ratio of ~3 between the X (horizontal) and Y (vertical) planes.

To obtain mass resolution an m/q dispersion is provided, with the consequence that only part of the charge state distribution of the reaction products can be transmitted. Yet, being a full spectrometer (as opposed to a mass separator), CAMEL provides a focal plane large enough to include several charge state values (within about ±7% of the reference value m_0/q_0 of the central trajectory) with reasonable resolution and efficiency. For particles of one mass 2 to 4 adjacent charge states are transmitted for $8^+ < \bar{q} < 31^+$, depending on the actual $\bar{q}$ value.

The mass resolution ranges from ~1/200 to ~1/550, depending on the focal plane position along the longitudinal axis, selectable within a range of ~80 cm, and on the angular and energy distribution of the transmitted particles.

Several detectors are used with the spectrometer: at the focal plane the main detector is a combination of a multiwire proportional counter (MW-PPAC) and a Bragg Chamber in the same gas volume [17]. Measured parameters are: X, Y, E, BP (ΔE), t. The MW-PPAC area is 14×14 cm^2 and the Bragg Chamber is cylindrical with internal diameter of 15 cm.

At the present time an entrance window to the F.P. detectors of 12×7 cm^2 is used, consequently the focal plane width is restricted to 12 cm out of the 15 cm maximum available extension.

Fig. 6 shows the X and Y profiles of the focal plane image obtained from the MW-PPAC with the reaction ^{64}Ni + ^{64}Ni at E_{beam} = 216 MeV: three charge states are accepted in this case for all the principal evaporation residues, and a mass resolution of ~1/300 is observed.

Around the target position it is possible to set four γ-detectors (Ge or NaI), at a distance of ~15 cm from the target, and small Si-detectors inside the reaction chamber, at various angles.

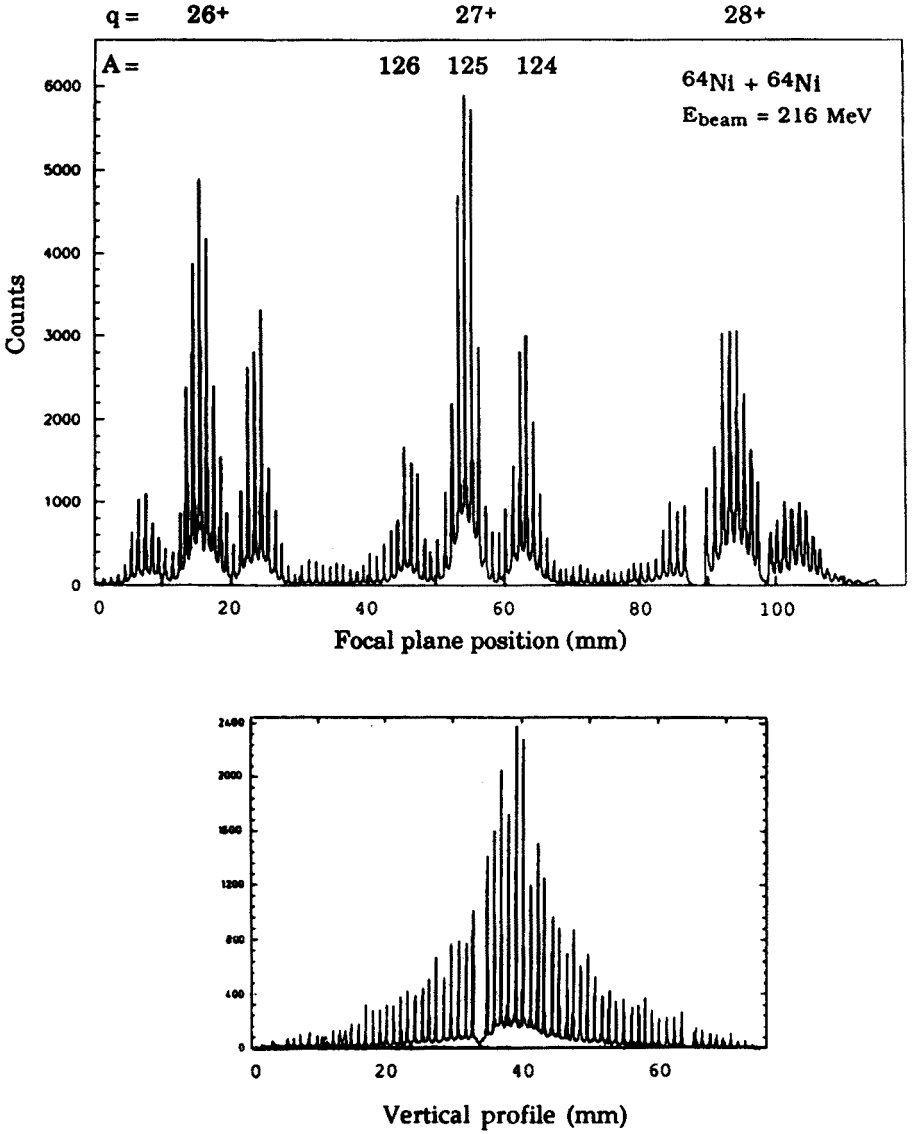

Fig. 6. CAMEL focal plane image in the horizontal (dispersion) and vertical planes, obtained with a MW-PPAC detector (a few wires are missing) having a front window of 12 cm horizontal × 7 cm vertical size. The solid angle accepted into CAMEL is ~7.5 msr, limited by a diaphragm.

3. Fusion Cross Section Measurements.

Efficiency and sensitivity are the two aspects, of particular interest for measurements of fusion cross section around the Coulomb barrier, that will be discussed below.

Due to momentum conservation the fusion-evaporation products are naturally focused around the beam direction, therefore the spectrometer is used at 0° for the maximum efficiency. The set-up for the cross section measurements includes the following detectors:

- MW-PPAC + Bragg Chamber at the focal plane;
- one (two) Si-detector(s) placed at an angle θ ($\pm\theta$, right and left) with respect to the spectrometer axis and ~13 cm from the target, used to measure the Rutherford scattering for beam monitoring purposes;
- one Ge detector close to the target (90° to the beam direction in the examples shown below), used to measure the efficiency of the spectrometer set-up, as described in the following.

The cross section is obtained from the expression:

$$\sigma_{Fus} = \frac{N_{Fus}}{N_{Mon,\theta}} \times \left(\frac{d\sigma}{d\Omega}\right)_{R.,\theta} \times \frac{\Delta\Omega_{Mon}}{\varepsilon}$$

where N_{Fus} represents the fusion events detected at the focal plane after proper background subtraction, $N_{Mon,\theta}$ the elastic scattering events detected at the angle θ by the monitor detector in the same time interval, $\Delta\Omega_{Mon}$ the monitor solid angle, $(d\sigma/d\Omega)_{R.,\theta}$ the Rutherford cross section at the angle θ and ε the total efficiency of the fusion events detecting system (including the effect of the limited angular acceptance of the spectrometer).

It is possible to evaluate in a direct experimental way the total efficiency ε by using a Ge detector close to the target and by recording the γ-spectra with and without a coincidence condition with the focal plane detector; the ratio between the photopeak intensities of characteristic γ-transitions in the principal evaporation residues in the 2 γ-spectra directly provides ε :

$$\varepsilon = \frac{N_{\gamma coinc.}}{N_{\gamma sing.}}$$

The absolute measurement of the efficiency through the observation of characteristic γ-rays is directly related to the production of the nuclear residues,

therefore it includes all of the efficiency reduction causes, in particular, as already mentioned, also the effect of the angular distribution of the ions.

In some cases significant differences may be observed between the efficiency values obtained from the various exit channels, as identified by the characteristic γ-transitions: these differences may be caused by large variations of the space and energy distributions of the recoils (e.g. between neutron and alfa emission channels) or by the existence of isomeric states, which usually decay via electron conversion therefore modifying the charge state distribution of the recoils. In this last case the q distribution, besides being shifted to higher q values, is also usually broadened, with less intensity left per charge state, and the transmission efficiency is therefore reduced.

In all cases a measurement of the distribution of particles with respect to the involved parameter (angle, energy or charge state) can be performed, if needed, by making proportional changes in the electric and magnetic fields of the spectrometer or by rotating the instrument around the target and allows to take into account possible exit-channel effects. In the case of isomers the problem can be sometimes eliminated by positioning a thin (10-20 $\mu g/cm^2$) carbon foil downstream of the target to restore the equilibrium charge state distribution, provided the isomeric state decays within the ~13 cm available between the target and the farthest possible carbon-foil position. An example is shown in fig. 7, for the fusion reaction of ^{33}S (170 MeV) + ^{124}Sn [18], where the ionic charge state distributions, measured with CAMEL, can be compared with and without the carbon foil in position. Of course, in the extreme case of isomers that decay well inside the spectrometer the corresponding signal is lost or contributes to the background.

As only the most prominent lines in the γ-spectra are used in this procedure of efficiency measurement the resolution of the Ge detector does not need to be much refined and, also, the low efficiency of a single detector can be accepted.

The transmission efficiency of CAMEL is essentially determined by the angle, energy, mass and charge-state distributions of the fusion-evaporation products, therefore large variations are expected depending on the particular reaction kinematic. The fusion reaction of ^{64}Ni + ^{64}Ni represents a favourable case because of three reasons: strong forward focusing of the products in the laboratory frame caused by beam-target symmetry, main fusion-evaporation channels corresponding to neutron emission only and no evidence of the existence of isomeric states. Preliminary results are available from the analysis of experiments recently performed using this reaction: in this case the total

efficiency ε has been measured at energies around the Coulomb barrier using the two most intense transitions in ^{124}Ba and ^{125}Ba, obtaining $\varepsilon \approx 0.21 \pm 0.03$.

It is interesting to compare this result with an analytic determination of the spectrometer transmission.

The efficiency ε can be seen as the product of two components, corresponding to the transmission efficiency of the spectrometer itself and the efficiency of the particle detection system: $\varepsilon = \varepsilon_{CAMEL} \times \varepsilon_{Det}$. To determine ε_{CAMEL} separately it is necessary to calculate or measure the angle, energy, mass and charge-state distributions of the fusion-evaporation products.

The energy distribution is calculated to be about ±7% FWHM and is therefore practically entirely contained within the spectrometer acceptance throughout the used focal plane interval of 12 cm. Fig. 8 shows an example of focal plane bidimensional spectrum E vs X, where the energy extent of the spots corresponding to each mass value is sensibly constant along the X range, i.e. for the three charge states displayed.

The angular distribution (fig. 9a), measured with a reduced aperture of ±0.65° in both planes at the entrance of the first quadrupole lens, shows that already at 3° the intensity is reduced below 5% of the maximum; the transmission obtained, from this distribution, for an entrance aperture of ±3° horizontal and ±2° vertical ($\Omega \cong 7.5$ msr), as used in the experiment, is 85%.

The main cut in the transmission is caused, in this case, by the ionic charge state distribution. This distribution can be measured with CAMEL by setting all the electric and magnetic fields to values corresponding to the maximum transmission (central position) of each charge state, sequentially. The result is shown in fig. 9b: three sets of data are obtained from the observed intensities of the three groups (left, central and right charge state in the PPAC, see fig. 6). The three most abundant charge states add to a 40% of the total intensity (as is also expected from theoretical calculations). From fig. 9b it can be also observed that the three distributions (which are not normalized) are practically coincident, except for the right q being slightly weaker, indicating a rather flat transmission along the used portion of the focal plane (12 cm), for this reaction.

Assuming that the variables are independent, which is a good enough approximation in this case for the purpose, by multiplying the partial transmissions an efficiency $\varepsilon_{CAMEL} \cong 0.34$ is obtained. The difference between the measured total efficiency ($\varepsilon = 0.21$) and the geometrical efficiency of CAMEL ($\varepsilon_{CAMEL} = 0.34$) indicates for the focal plane detector system: $\varepsilon_{Det} \cong 62\%$.

The sensitivity is controlled by reduction and discrimination of the background at the focal plane; this background is essentially caused by beam

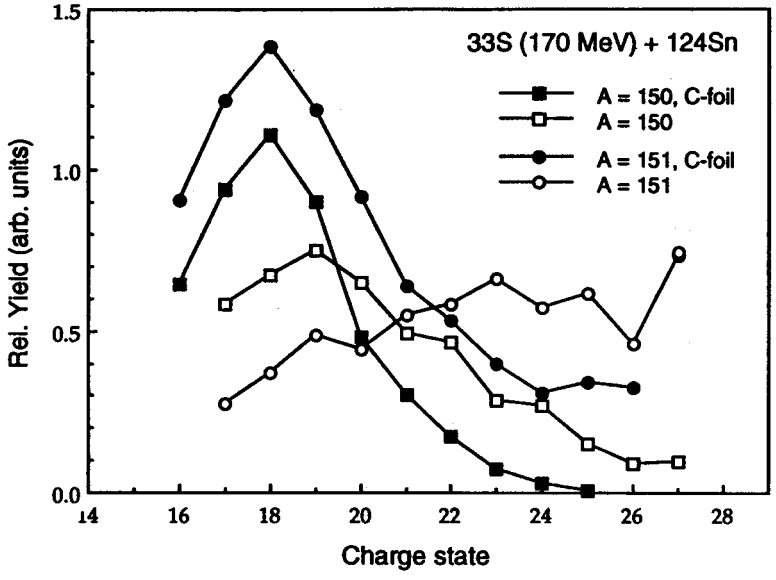

Fig. 7. Ionic charge state distributions measured with CAMEL with and without a 10 $\mu g/cm^2$ carbon foil positioned ~13 cm downstream of the target.

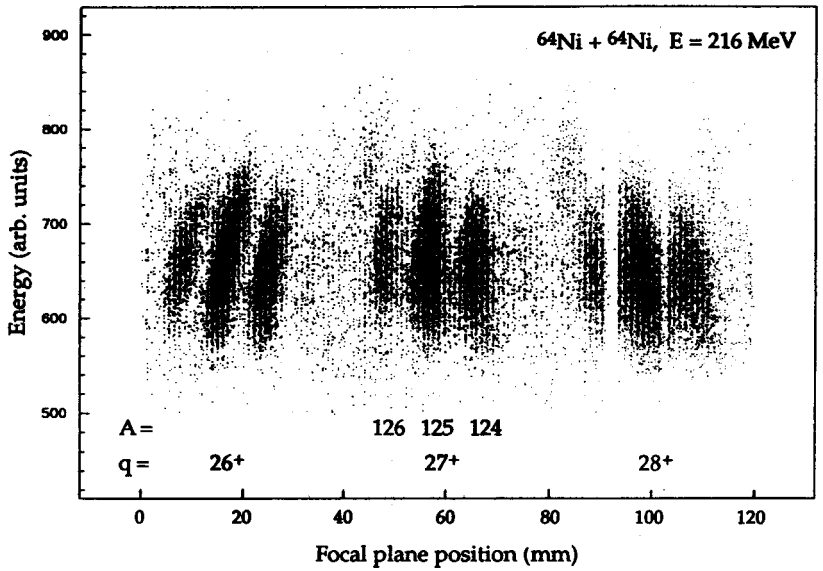

Fig. 8. Scatter plot of evaporation residues energy versus focal plane position, or m/q, in the same conditions of fig. 6.

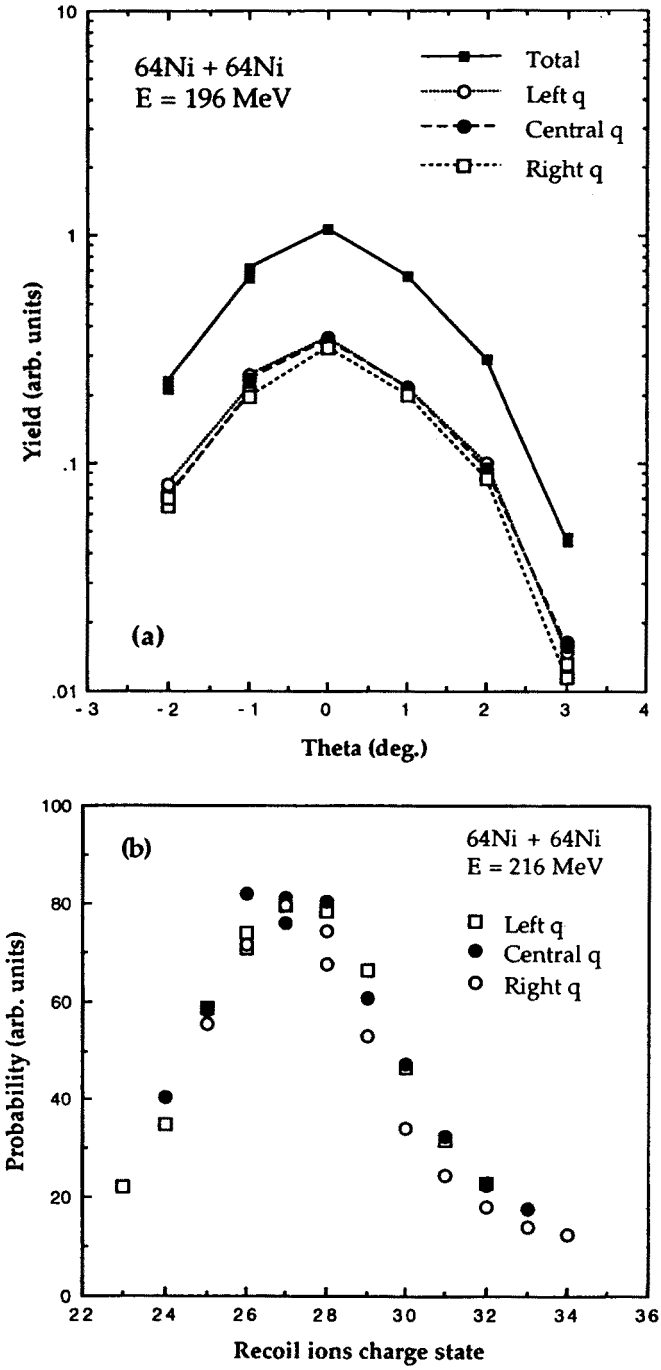

Fig. 9. Angular distributions (a) and charge state distributions (b) of fusion-evaporation residues from the indicated reactions at CAMEL focal plane. Left, central and right q refer to charge state groups as seen in fig. 6.

particles transmitted through the target and then dumped and scattered at the anode of the first electrostatic dipole. As described above the scattered beam is firstly rejected by the filtering action of the spectrometer itself, but, due to the large acceptance, this "hardware" rejection is, at 0° to the beam direction, generally not sufficient and some additional, "software", discrimination mean is needed.

The physical separation of the scattered beam is basically realized by the electrostatic dipole fields and therefore depends on the ratio $R = (E/q)_b/(E/q)_{ER}$ between the electric rigidities of the beam and fusion-evaporation particles. Symmetric reactions like the exemplified $^{64}Ni + ^{64}Ni$ are of course unfavourable from this point of view, showing, at 0°, suppression factors around 10^7+10^8 with $R \approx 2.5$. For comparison, at $R \approx 3.5$ the suppression factor improves by one order of magnitude.

The most efficient "software" method to separate the residual background results to be the measurement of the time of flight (ToF) of particles through the spectrometer (path length $l \approx 766$ cm) versus their energy. To preserve the operation at 0° the timing signal at the entrance of CAMEL is obtained by beam pulsing; the signal at the exit is provided by the PPAC detector. In practice, the PPAC is used as "start", to reduce the load on electronic modules, and a delayed pulsed-beam RF signal as "stop".

The ToF depends on the energy through the classical expression: $t = \sqrt{ml^2/2} \times 1/\sqrt{E}$, or, in our case: $t_D - t = t_D - \sqrt{ml^2/2} \times 1/\sqrt{E}$, t_D being the stop delay, here considered with respect to the reaction time; in the plane (t_D-t, E) this relationship describes "parabola-like" curves (fig. 10). For each energy value the time difference depends only on the mass, being the path l very closely the same (within ≈10% at maximum) for each particle which originates at the target and reaches the focal plane after a few scattering events. A set of curves corresponding to the different mass values is observed. The resolution is quite adequate to separate beam-like from fusion-evaporation particles. The separation, depending on the ratio m_{ER}/m_{beam}, is obviously better for directly asymmetric reactions, as shown in fig. 11 (t_D-t is also commonly named ToF).

As anticipated, the sensitivity is therefore higher for situations (directly asymmetric reactions) for which the efficiency is lower because of less forward focusing of the particles of interest.

For the exemplified symmetric fusion reactions of $^{58,64}Ni + ^{64}Ni$ cross sections as low as a few tens of μbarns have been measured.

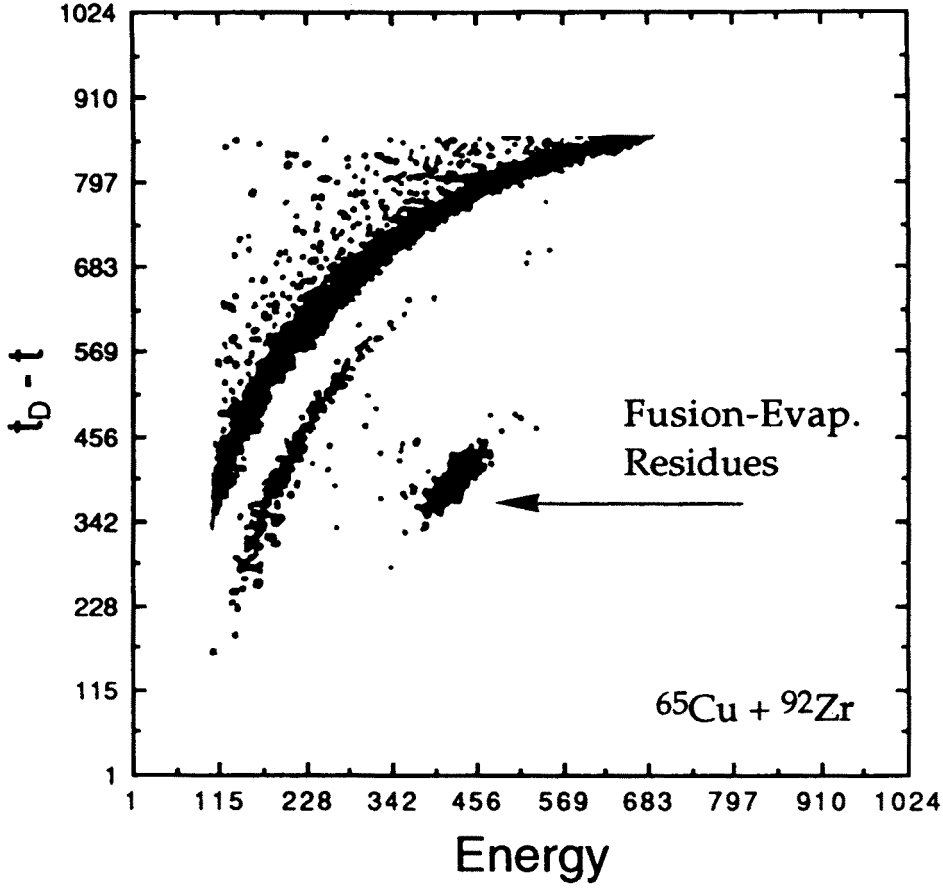

Fig. 10. Separation of fusion products by a time of flight versus energy measurement (see text).

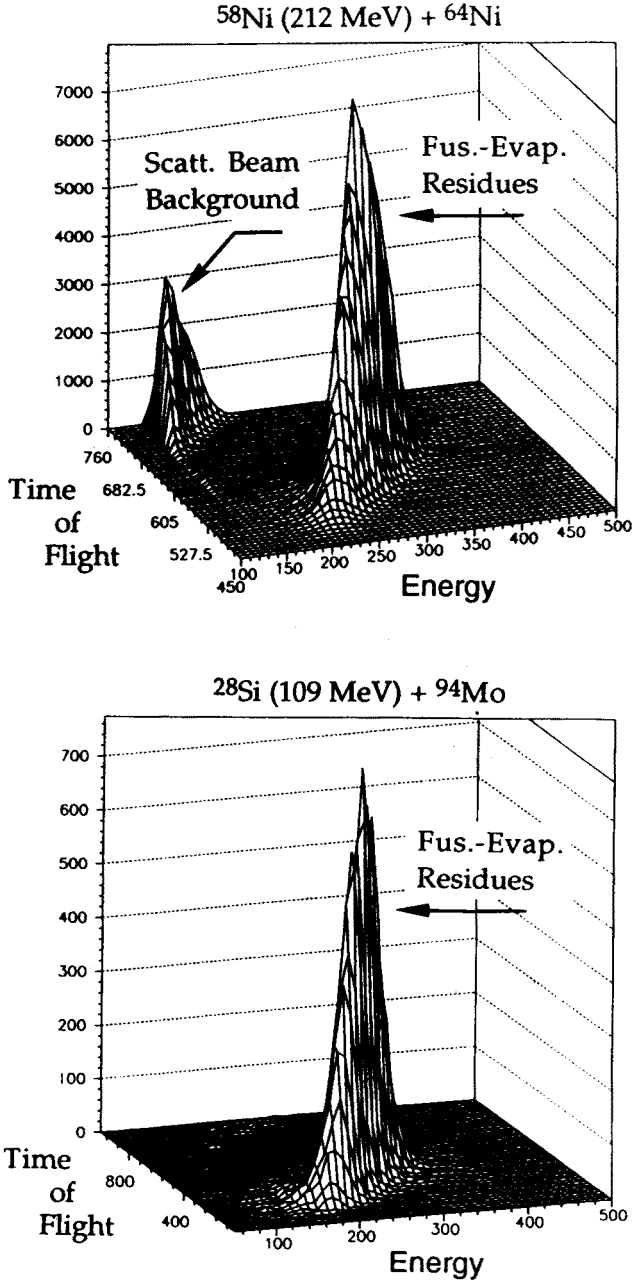

Fig. 11. Separation of fusion products from the scattered beam background by ToF versus energy measurement with CAMEL, for reactions with different mass asymmetry.

4. Gamma multiplicity measurements.

As most of the excess angular momentum of the compound nucleus is removed by γ-rays emitted by the evaporation residues the measurement of γ-rays average multiplicity $<M_\gamma>$ can be used to deduce the initial average angular momentum <l>. At energies around and below the Coulomb barrier the fusion γ-multiplicity is measured in the presence of a strong background produced by competing reaction channels like transfer and Coulomb excitation, therefore a clean identification of the fusion channel is essential. The tagging provided by a Recoil Mass Spectrometer (RMS) or various types of separators can be advantageous with respect to characteristic γ-rays tagging in that it is essentially independent on the particular decay scheme (isomeric states may be problematic for both methods) and tendentially more sensitive (fig. 12, [8]). The use of recoil mass spectrometers, like CAMEL, instead of simpler separators, because of the m/q dispersion provides information on separate fusion channels, at the expenses of some loss of efficiency caused by the q dispersion of the products, as discussed in the previous chapter.

The <l> can be calculated through the following expression:

$$<l> = \Delta I_{\gamma ns} \times (<M_\gamma> - M_{\gamma s}) + \Delta I_{\gamma s} \times M_{\gamma s} + \Delta I_{n,p} \times M_{n,p} + \Delta I_\alpha \times M_\alpha + <I_{g.s.}>$$

where the five terms correspond, in the sequence, to the angular momentum carried away by non-statistical (index γns, $M_{\gamma ns} = <M_\gamma> - M_{\gamma s}$) and statistical (index ns) gamma rays and by particles (index n, p, α), and to the weighted sum of the ground state angular momenta of the residual nuclei. In practice difficulties may arise from various problems: existence of isomeric states that prevent the observation of underlying γ-transitions and often also the detection of corresponding residual nuclei, unsufficient knowledge of the decay scheme, internal conversion events, determination of the particle multiplicities and loss of sensitivity for low-energy transitions. The definition of the parameters used in the above expression usually requires some assumptions and approximations that fit the particular case under study [3], [7], [8], [19].

The described apparatus has been used to measure the $<M_\gamma>$ by adding 4 NaI detectors (4" × 4") around the target position, at ~20 cm from the target, with a total efficiency of 3.3% and using the expression:

$$< M_\gamma > = \frac{N_{Fus.,coinc.}}{N_{Fus.,sing.}} \times \frac{c_n}{\varepsilon_{NaI}},$$

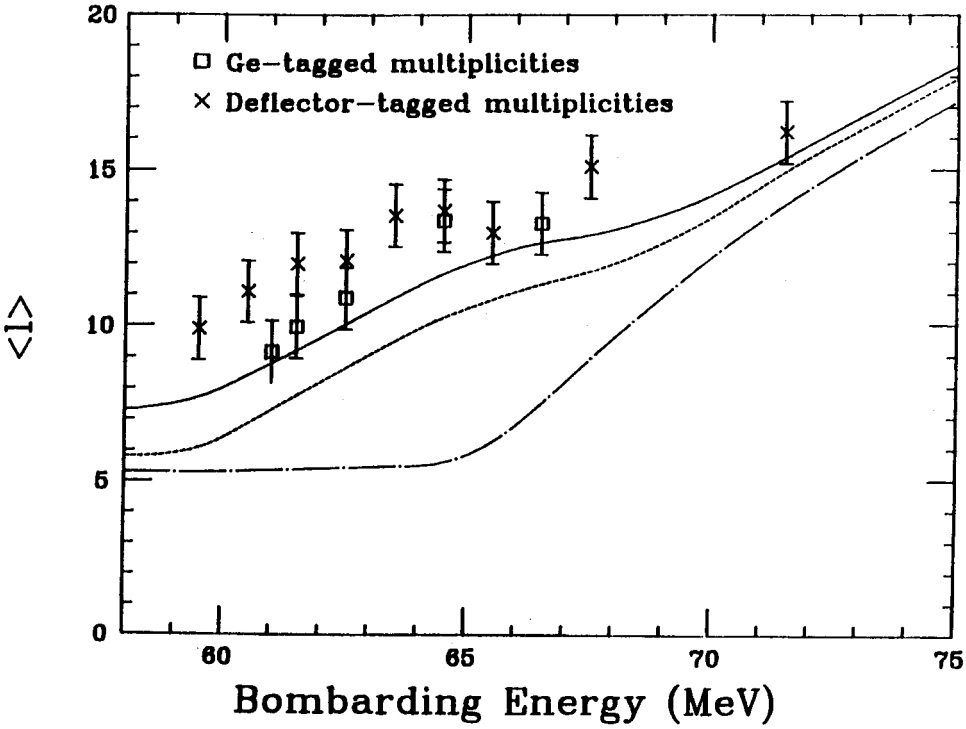

Fig. 12. Average angular momentum for $^{16}O + ^{154}Sm$ as deduced from γ-multiplicity data obtained with two different tagging methods. Calculation predictions with and without channel coupling are also shown. [8].

which gives the average multiplicity as the ratio of the number of evaporation residues detected in coincidence with any NaI detector and the same number without the coincidence condition, with this ratio corrected for the efficiency ε_{NaI} of the γ-detectors and for the effect of the evaporated neutrons on the NaI detectors (c_n factor).

<Mγ> is, instead, independent on the efficiency of the evaporation residues detection set-up ($\varepsilon = \varepsilon_{CAMEL} \times \varepsilon_{Det.}$).

The mass spectrum provided by CAMEL can be used for the determination of the multiplicity of the emitted particles and percentage contribution to $<I_{g.s.}>$ of the various evaporation channels. In cases of non-negligible charged particles evaporation either the Z identification can be obtained by an energy-loss measurement at the focal plane or the particle multiplicities should be theoretically estimated.

By this method, the <Mγ> has been measured, for instance, for the systems $^{64}Ni + ^{64}Ni$ and $^{16}O + ^{112}Cd$. Preliminary results (fig.13, [20]) show evidence of sub-barrier enhancement of the <l> deduced distribution for the symmetric system, whereas this is absent in the case of the asymmetric system, which leads to the same compound nucleus ^{128}Ba.

5. Future Developments.

Associated with the fusion cross section and angular momentum "enhancements" observed for some heavy systems below the Coulomb barrier, a very broad spin distribution has been measured in some cases, extending to partial waves higher than predicted by standard fusion models [3], [7], [19]. Whether the experimental data are reproduced or not (experimental evidences are presented for both cases) by coupled channels or other theoretical formalisms, the information provided by the measurement of detailed spin distributions imposes stringent conditions on the model parameters and therefore represents an important test for the proposed theories.

Large arrays of γ-detectors provide efficiency and granularity sufficient to measure a distribution of multiplicities, from which a spin distribution can be deduced for the whole fusion reaction and for single gated channels. Fusion channel identification must be provided either by characteristic γ-ray or direct evaporation-residue tagging.

One array of 80 BGO crystals with a total efficiency of ~90% (combined with a second array of 40 Compton-suppressed HPGe), named GASP [21], [22], has recently started to operate at the L.N.L.; a schematic drawing of the apparatus is

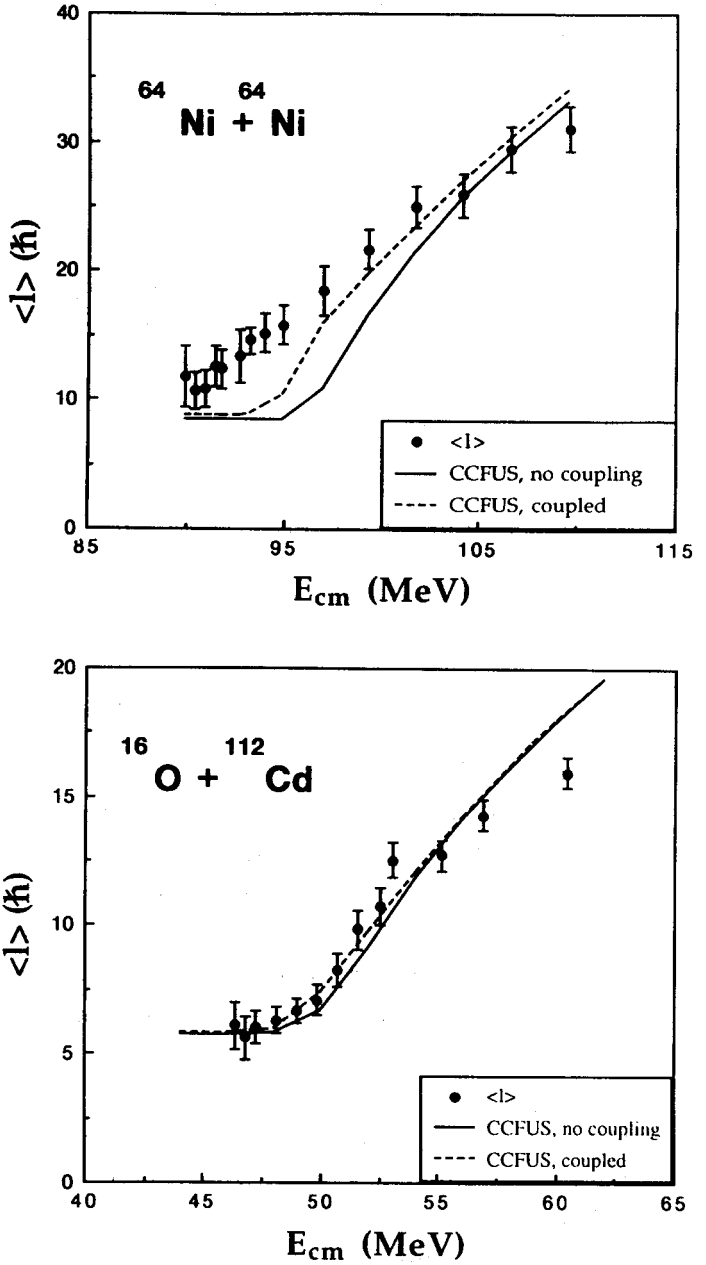

Fig. 13. Preliminary results for the average angular momentum as deduced from γ-multiplicities measured with CAMEL and 4 NaI detectors. Data are compared with simple coupled channel calculations.

shown in fig. 14. The combined use of GASP and CAMEL in coincidence experiments will provide a quite powerful tool to investigate sub-barrier fusion in a rather complete way.

Fig. 15 shows the geometry of the chosen coupling lay-out. Owing to the existing distribution of experimental apparatus in the west experimental room of the Tandem accelerator two alternatives were originally possible for linking the two spectrometers: temporary disassembling of GASP and reassembling of a limited number (perhaps one half of the total) of γ-detectors in the quite restricted space available in front of CAMEL on the -40°/-25° beam line (see fig. 15) or accepting a rather large separation between the unmodified GASP and the CAMEL platform, which entails an effective modification of the recoil spectrometer optical lay-out in the coupled operation.

The second choice was selected, which has the following main consequences:

- easy alternance of coupled and separate operation of the two facilities with a minimum of mechanical re-arrangement and time consumption;
- no restriction in the number of GASP detectors available for the coupled operation;
- no change in the CAMEL performance in the separate operation, but, in the coupled operation:
  - increased optical aberrations in the focal plane image of CAMEL due to the addition of a quadrupole doublet lens and a long drift;
  - reduction by a factor ~2 of CAMEL angular acceptance due to the longer distance (imposed by the geometry of the full GASP arrays) between the target position and the first magnetic quadrupole lens (70 cm instead of the 30 cm of the original CAMEL design).

In spite of the added drift and lenses the optical calculations show (fig. 16) that the CAMEL mass resolution can be kept very close to the usual levels, with the reduced solid angle, if the optical elements are used to "transfer" the added aberrations in the vertical, non dispersing, plane, as demonstrated by the larger vertical spot size of fig. 16b.

A short beam-test of CAMEL in the new geometry (i.e. with the target in the GASP centre position) has recently been performed. The mass resolution remains close to the original (fig. 17a), while the temporary presence of non-removable apertures in the original target area prevents, at moment, the evaluation of the transmission efficiency.

The background suppression via ToF (fig. 17b) is improved because of the longer path length: ~12 m instead of ~8 m. In addition, during γ-recoil

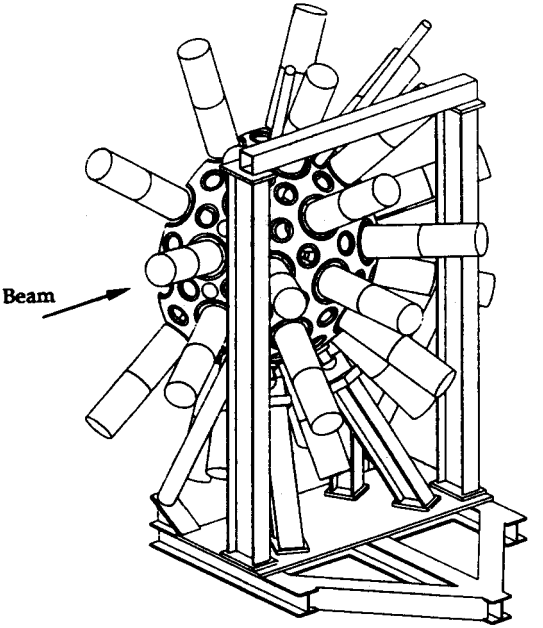

Fig. 14. Schematic view of the GASP apparatus: one half of the detectors array and supporting structure is shown.

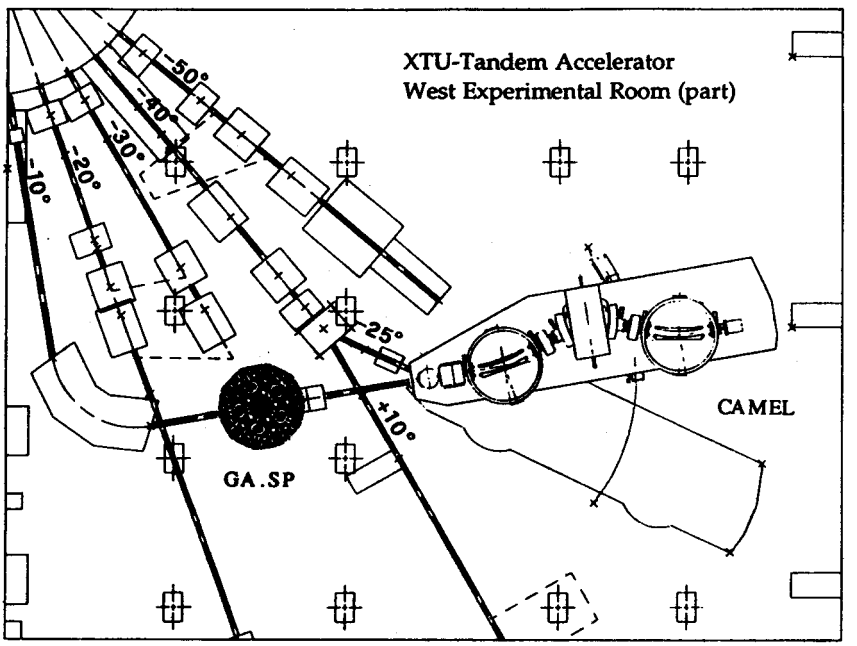

Fig. 15. Schematic lay-out of the GASP-CAMEL coupled system.

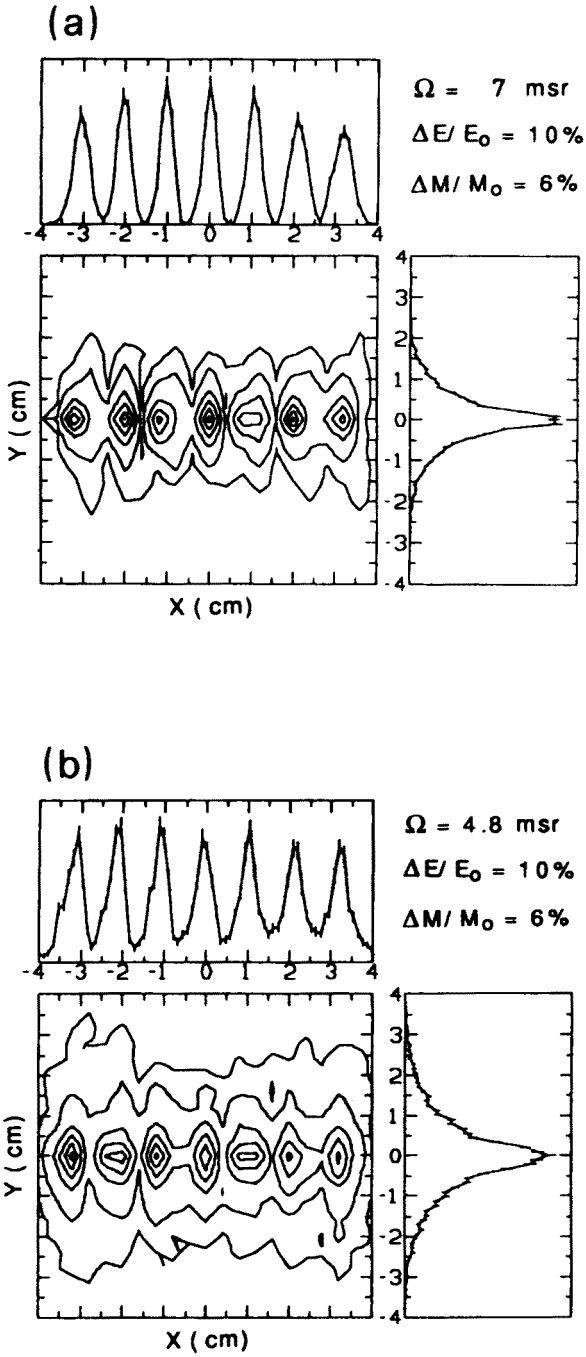

Fig. 16. Calculated CAMEL focal plane image with the target in the original (a) and new, GASP, position (b). Calculations are performed with the code GIOS [24].

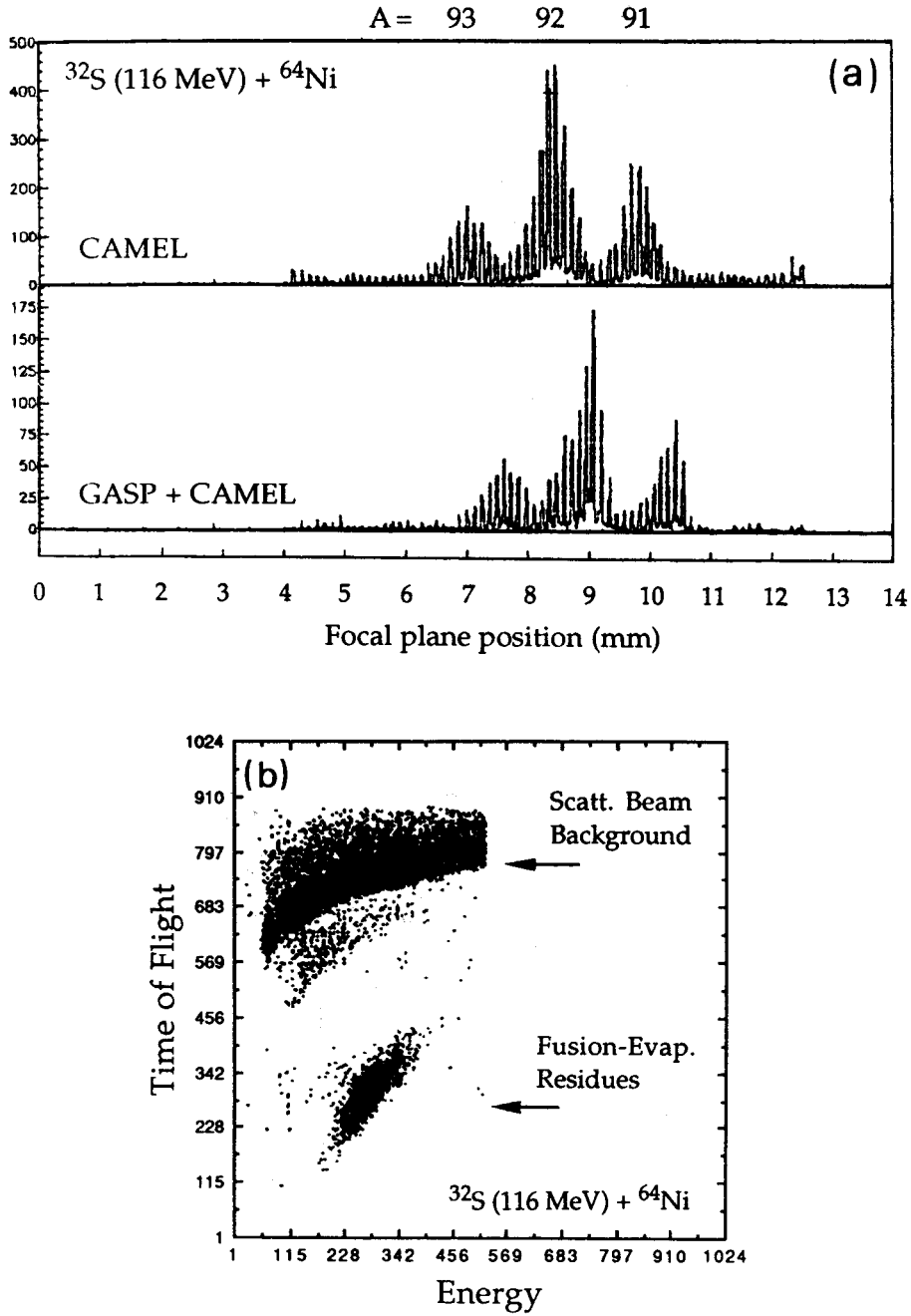

Fig. 17. Preliminary results of CAMEL performance in the coupled configuration: (a) m/q spectrum compared with the no-coupling situation; (b) fusion products separation via ToF versus energy measurement.

coincidence measurements it will be possible to use, for the ToF measurement, a time signal from the BGO ball to replace the pulsed beam RF signal (see chapter 3), with the obvious advantage of permitting the use of the Tandem DC beam.

The existence of a high resolution/high efficiency Ge array associated with the BGO array, besides providing an enormous widening of the possible research applications of the system, allows the comparison of the two tagging methods (via characteristic γ-rays or heavy ions detection) used to identify the fusion products and the choice of either one depending on the convenience in the different cases. As mentioned in the previous chapter and observed also in a similar situation during spectroscopic studies of fusion-evaporation residues [23], it seems that direct tagging on residual fusion products can be more sensitive particularly for weak reaction channels (as is the case of fusion below the Coulomb barrier) because of the favourable peak-to-background ratio of analyzed heavy ions with respect to individual lines in a γ-spectrum. However, tagging on characteristic γ-transitions can be more efficient particularly when isomeric states are present.

6. Conclusions.

Some peculiar features of the nuclear fusion reaction of heavy ions around and far below the Coulomb barrier has demonstrated to be a good test bench for our understanding of nuclear reaction dynamic and its correlation with nuclear structure and the description of the nuclear potential.

An experimental apparatus has been described which allows to perform at the same time measurements of different quantities (cross sections and angular momenta) of interest for sub-barrier fusion studies.

The main features of this set-up are:

- operation at 0° to the beam direction to match the typical forward peaking of fusion evaporation recoils, but also possibility of rotation to measure, e. g., angular distributions;
- mass identification throughout the nuclide chart to help in the identification of single reaction channels, particularly useful for calculating <l> on the base of the measured γ-multiplicities;
- very large acceptance, highly desirable for low cross section phenomena, with limitations for reaction products showing important e^--converted isomeric state decays;
- in spite of modest "hardware" beam rejection (consequence of large acceptance) isochronous trajectories allow a long time of flight path of 8 (12) m, ideal to

discriminate against unwanted particles and therefore to increase the sensitivity to weak reaction channels;
- possibility of connecting to the GASP γ-detector arrays in the next future;
- ample possibility of accomodating different types of detectors both for heavy ion detection (focal plane) and particle and gamma detection (target area).

Examples have been shown of recent operation of the system.

Acknowledgements.

The apparatus and experimental data here presented are the result of the hard work of many people. The contribution of all my co-authors on refs [16], [18], [20] is especially acknowledged. Dieter Ackermann and Fernando Scarlassara in particular have contributed to the analysis of shown data. I like to express special gratitude to James Daniel Larson for his precious collaboration and discussions while developing the design of CAMEL.

References.

[1] M. Beckerman et al., Phys. Rev. C25 (1982) 837.
[2] S. Gil et al., Phys. Rev. Lett. 65 (1990) 3100.
[3] A.H. Wuosmaa et al., Phys. Lett. B263 (1991) 23.
[4] C.H. Dasso et al., Nucl. Phys. A405 (1983) 381.
[5] C.H. Dasso et al., Nucl. Phys. A407 (1983) 221.
[6] R.A. Broglia et al., Phys. Lett. B133 (1983) 34.
[7] M.L. Halbert et al., Phys. Rev. C40 (1989) 2558.
[8] S. Gil et al., Phys. Rev. C43 (1991) 701.
[9] D.E. DiGregorio and R.G. Stokstad, Phys. Rev. C43 (1991) 265.
[10] M. Beckerman, Rep. Prog. Phys., 51 (1988) 1047.
[11] R. Vandenbosch, Ann. Rev. of Nucl. Sci., to be published.
[12] P.H. Stelson, Phys. Lett. B205 (1988) 190.
[13] N. Rowley, Nucl. Phys. A538 (1992) 205c.
[14] N. Rowley et al., Phys. Lett. B282 (1992) 276.
[15] R. Vandenbosch, Eighth Winter Workshop on Nuclear Dynamics, Jan. 1992, Jackson Hole, WY, USA.
[16] P. Spolaore et al., Nucl. Instr. and Meth. A238 (1985) 381.
[17] A. Guerrieri et al., Nucl. Instr. and Meth. A299 (1990) 133.

[18] L. Müller et al., Z. Phys. A341 (1992) 131.
[19] R.D. Fisher et al., Phys. Lett. B171 (1986) 33.
[20] D. Ackermann et al., Contribution Presented to the Int. Nuclear Physics Conference, Wiesbaden, Germany, July 26 - August 1, 1992.
[21] C. Rossi Alvarez et al., GA.SP Draft of the project, LNL Report 5/1989. INFN-L.N.L. Annual Report 1990: C. Rossi Alvarez et al., p. 160, and following.
[22] S. Lunardi, these proceedings.
[23] P.J. Ennis and C.J. Lister, Nucl. Instr. and Meth. A313 (1992) 413.
[24] H. Wollnik et al., GIOS - A Program for the Design of Ion Optical Systems, unpublished.